Multifrequency Time-Resolved Electron Paramagnetic Resonance Investigations after Photolysis of Phosphine Oxide Photoinitiators. Dependence of Triplet Mechanism Chemically Induced Dynamic Electron Polarization on Microwave Frequency

Timofei N. Makarov,[†] Anton N. Savitsky,[‡] Klaus Möbius,[‡] Dieter Beckert,[§] and Henning Paul*[,†]

Physical Chemistry Institute, University of Zurich, Winterthurerstrasse 190, CH-8057 Zurich, Switzerland, Institute of Experimental Physics, Free University of Berlin, Arnimallee 14, DE-14195 Berlin, Germany, and Interdisciplinary Research Group "Time-Resolved Spectroscopy", Faculty of Chemistry and Mineralogy, University of Leipzig, Permoserstrasse 15, DE-04318 Leipzig, Germany

Received: October 5, 2004; In Final Form: November 14, 2004

Phosphinoyl radicals were produced in benzene solution by photolysis of three acylphosphine oxide photoinitiators, diphenyl-2,4,6-trimethylbenzoyl phosphine oxide (**I**), bis(2,6-dimethoxybenzoyl)-(2,4,4-trimethylpentyl) phosphine oxide (**II**), and bis(2,4,6-trimethylbenzoyl) phenylphospine oxide (**III**). The chemically induced dynamic electron polarization (CIDEP) of the radicals was measured by time-resolved electron paramagnetic resonance spectroscopy at different microwave frequencies/magnetic fields, in S- (2.8 GHz, 0.1 T), X- (9.7 GHz, 0.34 T), Q- (34.8 GHz, 1.2 T), and W-bands (95 GHz, 3.4 T). The CIDEP was found to be due to a triplet mechanism (TM) superimposed by a radical pair mechanism comprising ST_0 as well as ST_- mixing. Contributions of the different CIDEP mechanisms were separated, and the dependence of the TM polarization on microwave frequency was determined. It agrees well with the numerical solution of the relevant stochastic Liouville equation, which proves the TM theory quantitatively. The applicability of previous approximate analytical formulas for the TM polarization is discussed. Parameters of the excited triplet state of **III** were estimated from the dependence of the TM polarization on microwave frequency. They are zero-field splitting constant 0.169 $cm^{-1} \leq D_{ZFS} \leq 0.195$ cm^{-1}, lifetime 40 ps $\leq \tau_T \leq$ 200 ps, and initial population of its T_z spin sublevel $0.92 \leq w_z \leq 1$.

Introduction

Radicals produced in solution by laser flash photolysis or pulse radiolysis usually exhibit nonequilibrium (non-Boltzmann) populations of their electron spin levels separated in a static magnetic field. The phenomenon is called chemically induced dynamic electron polarization (CIDEP). Over the last three decades, CIDEP has been investigated intensively both theoretically and experimentally.[1−5] Several mechanisms of CIDEP generation were proposed to explain the variety of experimental observations: the triplet mechanism (TM),[6,7] the radical pair mechanism (RPM),[8−10] the radical-triplet pair mechanism (RTPM),[11,12] and some others.[2,13] The CIDEP pattern exhibited by short-lived radicals can provide information on reaction mechanisms, interactions in radical pairs, radical spin dynamics, and reaction kinetics. Moreover, CIDEP improves significantly the sensitivity of time-resolved electron paramagnetic resonance (TREPR) spectroscopy, as the induced polarization can exceed that obtained in equilibrium by factors of 10−100.

One of the most important and common CIDEP mechanisms is the triplet mechanism (TM). It can arise in radicals, which are formed by rapid chemical reaction of a short-lived excited triplet state precursor. Very often, the intersystem crossing from a precursor's excited singlet to its triplet state is anisotropic, which leads to a nonequilibrium population of the electron spin sublevels of the triplet state precursor.[14] This nonequilibrium population is then transferred to the radicals produced by rapid chemical reaction of the triplet. The theory of the TM developed rather early[6,7] and has been used for qualitative CIDEP analyses in a number of experimental investigations[4,5] involving many chemical systems. Nevertheless, up to now quantitative proof of the theory is scarce. Experimental results were explained only qualitatively, mainly because of two reasons: (i) typically, several mechanisms contribute to the CIDEP pattern of a given chemical system, and it is hard to separate the TM from other contributions; (ii) it is difficult to determine the observed polarization quantitatively. To our knowledge, there has been only one semiquantitative study of the frequency dependence of the TM carried out by Ohara et al.[15] The authors utilized several EPR bands in the low microwave frequency region (X-, S-, and L-bands) to check the frequency dependence of relative changes of the TM polarization normalized to the ST_0 RPM contribution. The relative change of the TM polarization (increase or decrease) was found to agree qualitatively with predictions of the theory developed by Atkins and Evans.[6]

In this work, we examine for the first time quantitatively the dependence of the TM polarization on microwave frequency/magnetic field over the low and high frequency region. For this purpose, four electron paramagnetic resonance (EPR) bands were utilized to cover a broad microwave frequency/magnetic field range: S-band (2.8 GHz, 0.1 T), X-band (9.7 GHz, 0.34 T), Q-band (34.8 GHz, 1.2 T), and W-band (95 GHz, 3.4 T). This allowed us to separate different CIDEP contributions and

* Corresponding author. Fax: +4116356856. E-mail: hepaul@pci.unizh.ch.
[†] University of Zürich.
[‡] Free University of Berlin.
[§] University of Leipzig.

10.1021/jp0454725 CCC: $30.25
Published on Web 02/19/2005

SCHEME 1

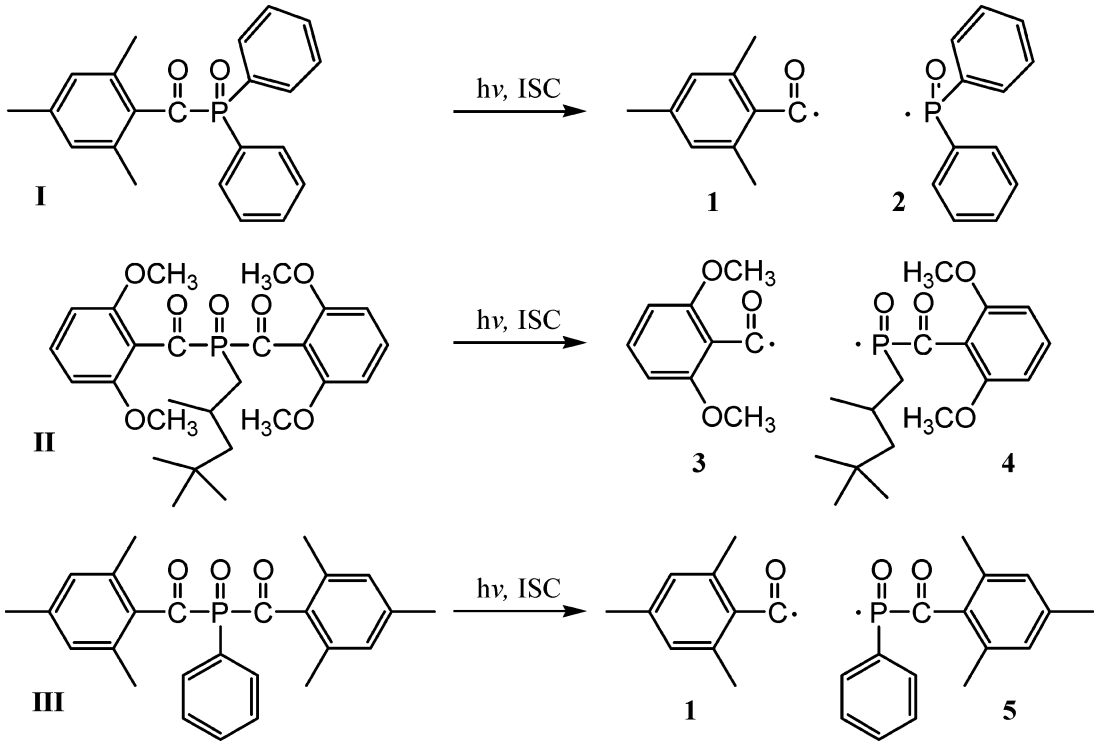

SCHEME 2: Reaction Scheme for the Primary and Secondary Steps of the Photolysis of the Acylphosphine Oxide Photoinitiators

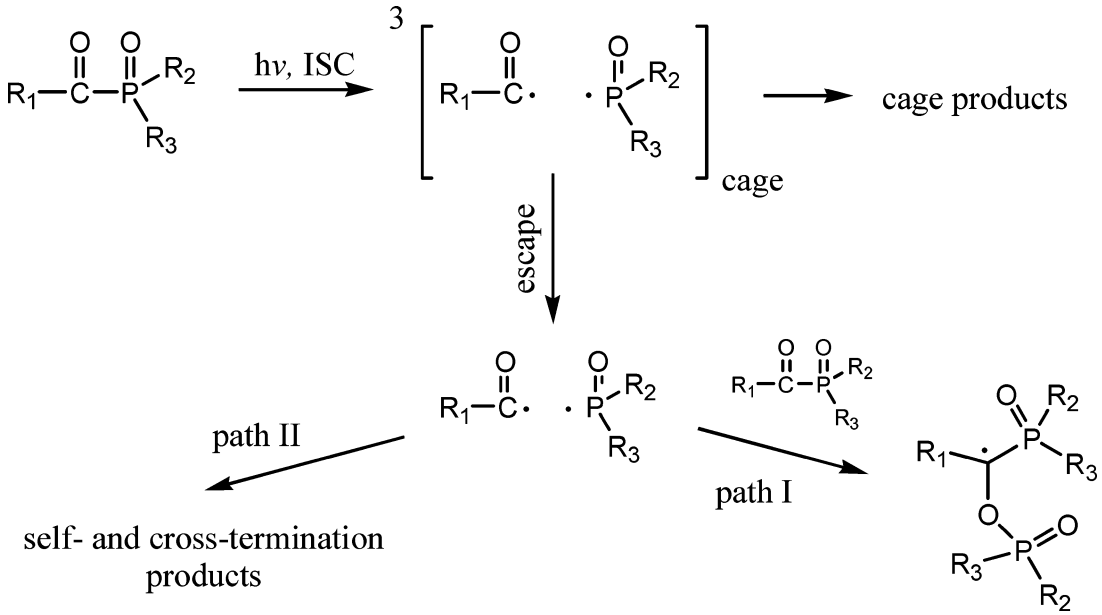

to obtain TM polarizations in absolute units, which could be directly compared with the TM theory.

The dependence of the TM polarization on the microwave frequency was studied for phosphinoyl radicals produced by photolysis of acylphosphine oxides. Acylphosphine oxides belong to an important class of polymerization photoinitiators. They have been widely investigated, and therefore, a lot of the relevant parameters are known for these compounds. In this paper, three acylphosphine oxides have been examined (Scheme 1): diphenyl-2,4,6-trimethylbenzoyl phosphine oxide (**I**), bis-(2,6-dimethoxybenzoyl)-(2,4,4-trimethylpentyl) phosphine oxide (**II**), and bis(2,4,6-trimethylbenzoyl) phenylphospine oxide (**III**). The photoreaction mechanisms of these molecules are known from literature[16,17] and are summarized in Scheme 2. Photolysis of **I**, **II**, and **III** yields benzoyl and phosphinoyl radicals via α-cleavage of a short-lived (τ_T < 1 ns) excited triplet state, formed from the photoexcited singlet state of the parent compounds via intersystem crossing (ISC). The high quantum efficiencies of the radical-forming reactions[17,18] (Φ > 0.5), the well-suited light absorption properties in the near-UV (ϵ(355 nm) = 260 (**I**), 1050 (**II**), and 650 (**III**) M^{-1} cm^{-1} in benzene), and the stability toward hydrolysis have established them as commercial initiators for light-induced radical polymerization.[16,17] The primary and secondary reaction steps of **I**, **II**, and **III** without (Scheme 2, paths I and II) and in the presence of a variety of unsaturated compounds have been the subject of a

number of studies and are now fairly well understood.[16−22] Therefore, **I**, **II**, and **III** are attractive model systems for quantitative CIDEP studies.

Phosphinoyl radicals produced in the photolysis of **I**, **II**, and **III** possess readily recognized and analyzed doublet EPR spectra, well separated from the lines of other species. A simple doublet of tens of millitesla arises because of the strong hyperfine coupling between the odd electron and the ^{31}P nucleus (A(P) ≈ 25−40 mT) and only weak and unresolved couplings with other magnetic nuclei.[20,21,23] Previous time-resolved X-band EPR investigations after photolysis of **I**, **II**, and **III** have shown strong CIDEP effects.[20,21,23] It is known that phosphinoyl radicals produced by photolysis of these compounds carry strong absorptive polarizations due to the TM, which are superimposed by multiplet-type polarizations due to the RPM.

The compounds **I** and **II** were chosen because all of the parameters of their excited triplet states, which are relevant for the TM, are known (Table 3). Thus, the theory of the TM can be directly checked. In the last compound, **III**, the parameters of the excited triplet state are not known and have been determined here from the microwave frequency dependence of the TM polarization.

Experimental Section

All experiments were carried out at room temperature in benzene solutions. The reagents **I**, **II**, and **III** were obtained from Ciba Speciality Chemicals Inc. and used as supplied. Benzene was purchased from Fluka in its purest commercially available form and used without further purification. Sample solutions were deoxygenated by purging with helium or argon for 30−40 min prior to measurements. The initial concentrations of the reagents were chosen so that the optical densities of the solutions were kept within 0.5−1.0. In all experiments, we have attempted to keep the radical concentrations equal (below 10^{-4} M). All continuous wave electron paramagnetic resonance (cw-EPR) spectra and time profiles were recorded and analyzed at several microwave powers.

W-Band. The W-band TREPR experiments were performed in Berlin with a laboratory-built high-field EPR spectrometer operating at about 95 GHz with 10 ns response time.[24] A superconducting magnet (Cryomagnetics) provided a maximum field of 6 T. The sample quartz capillary, 0.6 mm i.d., was positioned along the axis of an optical transmission cylindrical TE_{011} cavity. The output of a Nd:YAG laser (Spectra Physics) operating at 355 nm was coupled into the cavity by means of a quartz fiber of 0.8 mm diameter. Laser pulse repetition frequency was generally set to 10 Hz, and the output energy was attenuated to a maximum of 1 mJ/pulse on sample surface. The sample solutions were pumped through the capillary by a motor-driven syringe with a flow rate of 0.6 μL/s to supply fresh sample material to the light-irradiated cavity volume after every six laser shots. The experiments were carried out at microwave field amplitudes up to $\omega_1 = 1.8 \times 10^6$ rad/s.

Q-Band. For time-resolved 34.8 GHz Q-band EPR measurements, the Fourier transform (FT) EPR spectrometer in Leipzig wasused. Laser photolysis of flowing sample solutions were carried out in a cylindrical quartz tube (0.8 mm i.d.) using a Lambda Physik excimer laser LPX105 (308 nm, 15 ns pulse width, 10−15 mJ/pulse). The power of the microwave pulses was 15 W with a $\pi/2$ pulse length of 80 ns. With the TH_{011} cavity used, the excitation width was about ±22 MHz. The real and imaginary parts of the free induction decay (FID) were detected by two quadrature channels with phase adjustment of 0°/90° and 180°/270° in the CYCLOPS mode (cf. ref 25 for the X-band equipment). The dead time of the FID was 60 ns. All FIDs were extrapolated into the dead time by the linear prediction singular value decomposition (LPSVD) method.[26] The complete spectra were measured by variation of the magnetic field offset. The number of repetitions per spectrum was in the range of 100−400. For all compounds, spectra were recorded at several time delays between the laser and the $\pi/2$ microwave pulse. The delays ranged from 30 to 200 ns with a step width of 10 ns.

X-Band. Our experimental setup for 9.7 GHz X-band TREPR measurements has been described previously.[27] It comprises a Nd:YAG (355 nm, 6 ns pulse width) or an excimer Compex 102 (308 nm, 20 ns pulse width) laser and an X-band cw-EPR detection system without field modulation (response time 90 ns). Sample solutions were exposed to laser irradiation (0.5−2 mJ/pulse on sample surface, 10 Hz repetition rate) while slowly flowing (5.5 μL/s) through a flat quartz cell (0.5−1 mm optical path length) inside a TE_{103} rectangular cavity. The experiments were carried out at microwave field amplitudes $\omega_1 = (0.5-3.5) \times 10^6$ rad/s.

S-Band. The setup for 2.8 GHz S-band TREPR measurements was based on the X-band device described above. A laboratory-made S-band microwave bridge together with a loop-gap resonator was installed instead of the corresponding X-band units. Response time of the S-band spectrometer was about 120 ns. Slowly flowing (5.5 μL/s) sample solutions were irradiated (0.5−1 mJ/pulse on sample surface, 10 Hz repetition rate) in a cylindrical quartz cell (1.9 mm i.d.). The experiments were carried out at microwave field strengths $\omega_1 = (0.5-3) \times 10^6$ rad/s.

Results

Photolysis of Diphenyl-2,4,6-trimethylbenzoyl Phosphine Oxide (I). W-, Q-, X-, and S-band transient EPR spectra after laser flash photolysis of **I** in benzene solution are shown in Figure 1. The spectra consist of three lines; the inner line stems from the carbon-centered benzoyl radical **1**, and the outer two are due to the phosphorus-centered diphenylphosphinoyl radical **2** (Scheme 1). From the W-band spectrum, the phosphorus hyperfine coupling, which splits the EPR spectrum of radical **2** in two lines, was determined as (36.25 ± 0.05) mT. This value is in good agreement with the previously reported X-band measurements (36.3 and 36.5 mT in toluene[22] and in benzene[20] solutions, respectively). The g values of the radicals **1** and **2** were obtained in the W-band as $g_1 = 2.00055 \pm 0.00005$ and $g_2 = 2.00412 \pm 0.00004$, respectively.

At short times after the laser flash, the W-band TREPR spectra of both radicals, **1** and **2**, exhibit a net absorptive polarization (Figure 1a). For the diphenylphosphinoyl radical **2**, an additional multiplet polarization of E/A type (low-field line in emission/high-field line in absorption) is superposed, which is well seen from the different intensities of the low- and high-field line. The net absorption observed for both radicals reflects the TM polarization transferred from the excited triplet state of **I**. In addition, the RPM is operative in the geminate triplet radical pairs (RPs) of **1** and **2**. It contributes a net polarization of the radicals via ST_0 mixing due to the different g values of **1** and **2** (Δg-RPM) and an E/A multiplet-type polarization via ST_0 mixing induced by the hyperfine splitting (ΔA-RPM). For the benzoyl radical **1**, the Δg-RPM contribution is positive (absorption), and for the diphenylphosphinoyl radical it is negative (emission) ($g_1 < g_2$). The initial polarization pattern of the radicals is different in all of the EPR bands (S-, X-, Q-, and W-bands), Figure 1. This difference is explained in terms

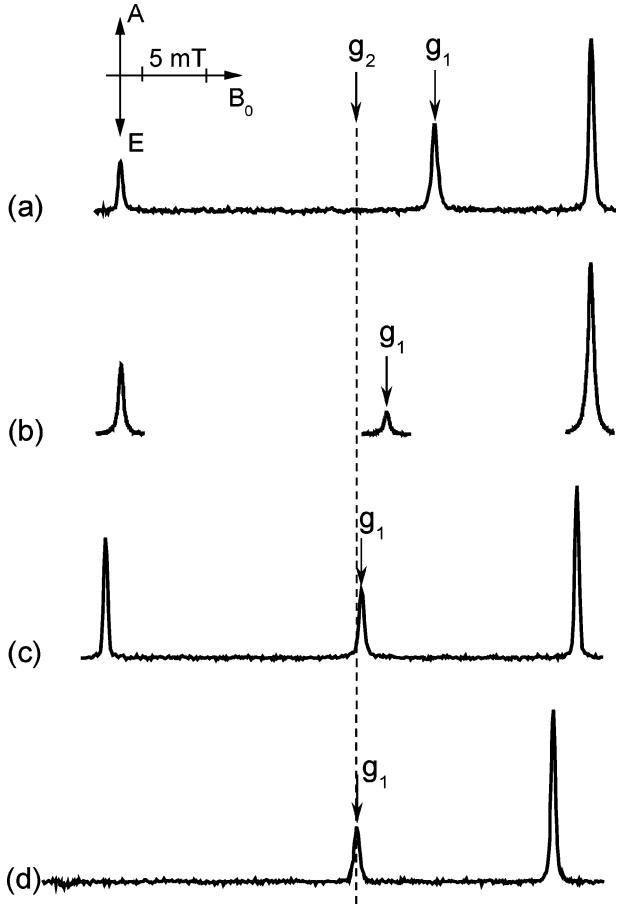

Figure 1. Transient EPR spectra recorded after laser flash photolysis of **I** in benzene at room temperature. (a) W-band TREPR spectrum accumulated in the interval 150−250 ns after the laser flash. (b) Q-band FT EPR spectrum recorded at 50 ns between the laser flash and $\pi/2$ microwave pulse. (c) X-band and (d) S-band TREPR spectra recorded 200 ns after the laser flash.

of the field dependence of the CIDEP generating mechanisms. For example, the multiplet ΔA-RPM polarization is, to a good approximation, magnetic-field independent,[28] whereas the polarization due to the Δg-RPM and TM changes[2] when going from W- to S-band EPR.

To investigate the CIDEP of the diphenylphosphinoyl radical system in more detail, the W-, X-, and S-band TREPR time profiles of the high- and low-field lines of **2** were compared, Figure 2, parts a, b, and c. The time profiles were analyzed in terms of net and multiplet contributions. Figure 2, parts d, e, and f, show the EPR kinetics of the net and multiplet polarizations, which were obtained by taking half the sum and half the difference of the intensities of the high- and low-field resonances of **2**, respectively.

At high magnetic fields (W-,Q-, and X-bands) the observed CIDEP evolution can be well-described by the CIDEP mechanisms mentioned above and the reaction Scheme 2. The initial net absorptive polarization from the TM and Δg-RPM decays with spin−lattice relaxation time T_1. The same does the multiplet polarization contribution that was initially gained in the geminate pairs of radicals **1** and **2** by the ΔA-RPM. At later times, the ΔA-RPM in F-pairs gives rise to a multiplet polarization due to the spin-selective terminations of the radicals (path II in Scheme 2). Because of the *g* factor difference of radicals **1** and **2**, there should also be a small production of net polarization at later times by the Δg-RPM in F-pairs of these two radicals. But this net contribution is small compared to the multiplet RPM polarization. Thus, as expected, in X-band the net EPR signal intensity decays faster than the multiplet EPR signal intensity (Figure 2e). The slow decay of the net polarization in W-band (Figure 2d) is attributed to the equilibrium radical polarization, which in first approximation is proportional to the strength of the external magnetic field and, therefore, is 10 times larger in the W- than that in the X-band.[24] In the X-band, the radicals in thermal equilibrium were not observed due to the high initial net polarization and the smaller equilibrium polarization.

At low magnetic fields (e.g., S-band), ST_- mixing in radical pairs (ST_- RPM) plays an important role for the phosphorus-centered radicals[29,30] in addition to the above-mentioned CIDEP mechanisms. The CIDEP effect due to ST_- transitions is dependent on the hyperfine component of the radical EPR spectra. Consider first F-pairs of two radicals **2**. In this case, the isotropic hyperfine-interaction-induced transition from the triplet $T_-(\beta_N\beta_N)$ spin sublevel of the RP to its singlet state S is suppressed because the total spin of the RP has to be conserved. At the same time, transitions from T_- with nuclear spin multiplicities $\alpha_N\beta_N$, $\beta_N\alpha_N$, and $\alpha_N\alpha_N$ to the singlet state are possible. As a result, the EPR component of radical **2** with parallel nuclear spin orientation (α_N) will be more emissively polarized than the EPR component with antiparallel nuclear spin orientation (β_N). Another possible F-pair is that formed of radicals **1** and **2**. This RP can be well considered as having only one (phosphorus) nucleus with spin $^1/_2$. Then only the mixing $T_-(\alpha_N) \leftrightarrow S(\beta_N)$ is induced by the isotropic hyperfine interaction. As a result, again the EPR component of radical **2** with nuclear spin orientation α_N will be emissively polarized, whereas the other component will show no polarization. In fact, the S-band measurements shown in Figure 2c clearly meet this ST_- mixing situation discussed above. The low-field line (parallel phosphorus nuclear spin orientation, α_N) of the diphenylphosphinoyl radical **2** shows a pronounced long-lived emission, whereas the high-field transition (antiparallel phosphorus nuclear spin orientation, β_N) has only some minor polarization at long times. A time behavior like that of the EPR signal intensities agrees with a ST_- RPM in radical F-pairs, which only adds emission to the low-field line and does not change the intensity of the high-field one. Obviously, the probability for formation of F-pairs composed of radicals **1** and **2** is appreciably higher than that for formation of pairs containing two radicals **2**. This is not unexpected, because radical **2** is much more reactive than **1**, especially with regard to the addition to the parent compound (path I in Scheme 2), which causes the concentration of radicals **1** in the solution to dominate.[17,20] Of course, the ST_- RPM contributes as well to the initial polarization of radical **2**, because the geminate radical pair is triplet and is formed from the radicals **1** and **2**. Thus, the ST_- RPM contributes to the initial polarization in radical **2** in the same way as in F-pairs of radical **1** and **2** (i.e., by an E + E/A polarization pattern with equal size of net and multiplet polarization). In radical **1**, the ST_- RPM creates an additional net emissive polarization.

From the time dependence of the net and multiplet EPR intensities (Figure 2, parts d, e, and f), the initial net/multiplet (P_n/P_m) ratios were obtained for W-, Q-, X-, and S-bands. These initial ratios P_n/P_m were estimated as limits of $P_n(t)/P_m(t)$ at zero time after the laser flash, $t \rightarrow 0$. For calculation, the time profiles of the net polarizations were divided by those of the multiplet polarizations, and the resulting, approximately linear, time dependencies $P_n/P_m(t)$ were then fitted by linear regression in the time range between 50 and 150−200 ns (the points between 0 and 40 ns were not considered because of bad signal/

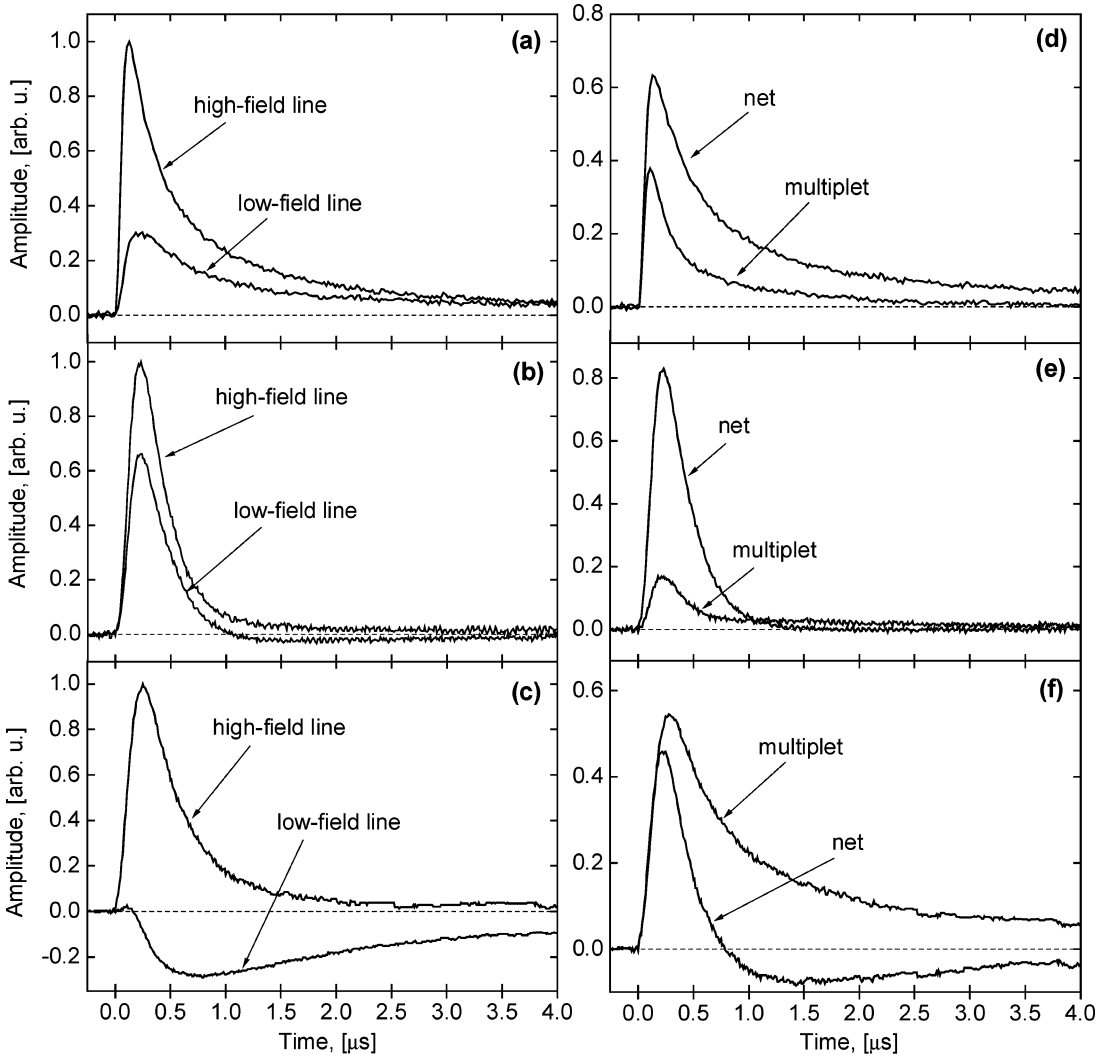

Figure 2. (a) W-band, (b) X-band, and (c) S-band high- and low-field line time profiles of the EPR signal amplitude of diphenylphosphinoyl radicals **2** after laser flash irradiation of **I**. (d) W-band, (e) X-band, and (f) S-band transient EPR kinetics of net and multiplet polarization of diphenylphosphinoyl radicals **2** obtained by taking half the sum and half the difference of respective high- and low-field time profiles. The amplitude of the signals is normalized to the maximum amplitude of the corresponding high-field line time profiles.

TABLE 1: Initial Net/Multiplet Polarization Ratios P_n/P_m of Phosphinoyl Radicals, 2, 4, and 5, Produced by Photolysis of I, II, and III, Respectively, in Dependence on the EPR Band

EPR band	**2**	**4**	**5**
S	1.02 ± 0.15	0.33 ± 0.03	1.93 ± 0.16
X	4.56 ± 0.35	1.55 ± 0.12	4.59 ± 0.48
Q	2.49 ± 0.18	1.00 ± 0.10	1.53 ± 0.11
W	1.55 ± 0.15	0.65 ± 0.05	1.00 ± 0.10

noise ratio at early times). The initial P_n/P_m ratios were found by linear extrapolation to $t \rightarrow 0$. This procedure was necessary especially in the S-band, because there the low- and high-field EPR transitions of radical **2** have different relaxation times.[31] For statistics, the ratios $P_n/P_m(t = 0)$ were determined from several time profiles recorded at different microwave field amplitudes ω_1. The values of the initial P_n/P_m ratios of radical **2** are presented in the first column of Table 1 in dependence on the EPR band.

In addition to the initial P_n/P_m ratio, also the absolute value of the initial polarization in the W-band experiment can be determined, because the initial signal can be scaled to the thermally equilibrated one, which is measurable in the W-band (Figure 2d). Also, kinetic information about radical reactions is obtainable directly from the analysis of the time dependence of the radical EPR intensity in the W-band. For the photolysis of **I**, it has been shown[24] that W-band EPR net polarization time profiles of the diphenylphosphinoyl radical **2** can be well analyzed by an analytical solution of the Bloch equation for the v magnetization

$$v(t) = P_{eq}[R]_0\omega_1 T_2[e^{-k_1 t} + (P_n - 1)e^{-t/T_1}] \qquad (1)$$

which is valid for $t > T_2$, if the conditions $T_2 \ll T_1$, $\omega_1^2 \ll T_1^{-1} T_2^{-1}$, and $T_1 k_1 \ll 1$ are fulfilled. T_1 and T_2 represent the relaxation times, ω_1 the microwave field amplitude, P_{eq} the radical equilibrium polarization, $[R]_0$ the initial radical concentration, and k_1 the first-order reaction rate constant with the parent compound **I** (path I, Scheme 2). P_n is the initial net polarization in units of the equilibrium polarization P_{eq}. The diphenylphosphinoyl radical system **2** was found to meet all of the above requirements in sufficient approximation under the conditions of the experiment.[24] Thus, according to eq 1, the decay of the net signal in the W-band can be simply analyzed in terms of two exponential decays. Therefore, eq 1 was convoluted with the response function of the W-band spectrometer and then fitted to the net signal of radical **2**, obtained in this work, varying k_1, P_n, T_1, and the amplitude. Optimal agreement with the experiment was found for $P_n = 8.5 \pm 1$, $T_1 = (600 \pm 50)$ ns, and $k_1 = (1.7 \pm 0.3) \times 10^5$ s^{-1}, in good

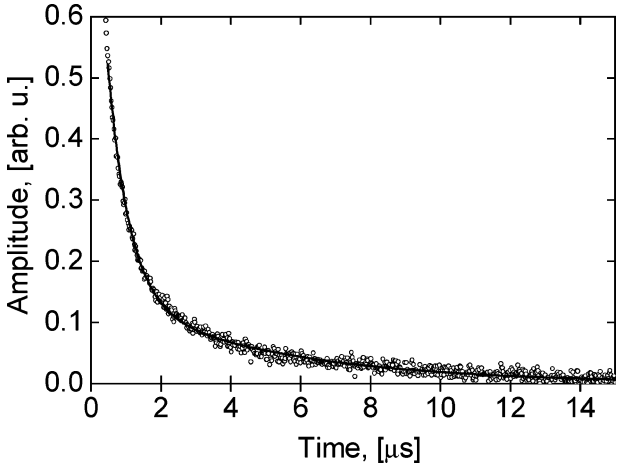

Figure 3. Net polarization time profile of radical **2** and least-squares fit with eq 1.

agreement with the results of the previous study.[24] The individual fits were obtained with reduced $\chi_2 \approx 1.1-1.4$, which demonstrates good quality of the data (Figure 3).

Thus, the radicals **2** are produced in the W-band with a net polarization $P_n = 8.5 \pm 1.0$, which corresponds to an initial population difference P_nP_{eq}(W-band) $= 0.066 \pm 0.008$. From the ratio $P_n/P_m = 1.55 \pm 0.15$ (Table 1) and $P_n = 8.5 \pm 1.0$, the initial W-band multiplet (E/A) CIDEP of radical **2** after photolysis of **I** is calculated as $P_m = (5.5 \pm 0.8)$, being equivalent to P_mP_{eq}(W-band) $= 0.043 \pm 0.006$ in terms of the population difference.

Photolysis of Bis(2,6-dimethoxybenzoyl)-(2,4,4-trimethylpentyl) Phosphine Oxide (II). W-, Q-, X-, and S-band transient EPR spectra after laser flash photolysis of **II** in benzene solution are similar to those obtained after photolysis of compound **I** (Figure 1S; Supporting Information). The inner line stems from the benzoyl radical **3**, and the outer doublet of triplets are due to the phosphinoyl radical **4** (Scheme 1). From the W-band spectrum, the phosphorus hyperfine splitting of radical **4** was determined as 27.29 ± 0.05 mT. This value is in good agreement with the previously reported X-band result[22] (27.3 mT in toluene solution). The g values $g_3 = 2.00057 \pm 0.00005$ and $g_4 = 2.00420 \pm 0.00004$ were obtained in the W-band for radicals **3** and **4**, respectively.

At short times after the laser flash, the W-, Q-, and X-band TREPR spectra of both radicals, **3** and **4**, exhibit a net absorptive polarization mainly due to the TM (Figure 1S, Supporting Information). For phosphinoyl radical **4**, a strong E/A type multiplet polarization, due to a ST_0 RPM, is present in addition to the net polarization. In the S-band an additional ST_- RPM contribution to the CIDEP pattern is observed. It results in an emissive polarization of the low-field line of the phosphinoyl radical **4** (Figures 1Sd and 2Sc; Supporting Information).

From the time dependence of the net and multiplet EPR intensities, the initial net/multiplet (P_n/P_m) ratios were obtained for radical **4** in W-, Q-, X-, and S-bands in the same way as for radical **2**. The values of the initial P_n/P_m ratios for **4** are presented in the second column of Table 1 in dependence on the EPR band.

Analysis of the decay of the W-band net polarization time profiles of radical **4** with eq 1 yielded the optimal values for P_n, T_1 and k_1: $P_n = 2.5 \pm 0.3$, $T_1 = 500 \pm 50$ ns, and $k_1 = (1.9 \pm 0.3) \times 10^5$ s^{-1}.

Thus, the radicals **4** are produced in the W-band with a net polarization $P_n = 2.5 \pm 0.3$, which corresponds to an initial population difference P_nP_{eq}(W-band) $= 0.020 \pm 0.002$. From P_n and the ratio $P_n/P_m = 0.65 \pm 0.05$ (Table 1), the initial W-band multiplet (E/A) CIDEP of phosphinoyl radical **4** after photolysis of **II** is calculated as $P_m = 3.9 \pm 0.6$, equivalent to 0.030 ± 0.005 in terms of the population difference.

Photolysis of Bis(2,4,6-trimethylbenzoyl) Phenylphospine Oxide (III). W-, Q-, X-, and S-band transient EPR spectra after laser flash photolysis of **III** in benzene solution also have the same structure as those observed after photolysis of **I** (Figure 3S; Supporting Information). Again, the inner line stems from the benzoyl radical **1**, and the outer two are due to the phosphinoyl radical **5** (Scheme 1). From the W-band EPR spectrum, the phosphorus hyperfine splitting of radical **5** was determined as 25.95 ± 0.05 mT, in agreement with the previously reported value[22] (25.8 mT, X-band, toluene solution). The g values are $g_1 = 2.00055 \pm 0.00005$ and $g_5 = 2.00400 \pm 0.00004$, respectively.

At short times after the laser flash, the W-, Q-, X-, and S-band TREPR spectra of both radicals, **1** and **5**, show a similar CIDEP pattern as that observed after photolysis of **I** and **II**. It was found that TM and ST_0 RPM contribute to the CIDEP of radical **5** in all bands and that the ST_- RPM contributes significantly only to the S-band spectra and time profiles (Figures 3S and 4S; Supporting Information).

Analysis along the lines discussed for radical **2** yielded for radical **5**, the initial net/multiplet (P_n/P_m) ratios presented in the third column of Table 1. Fitting of the decay of the W-band net polarization time profiles of radical **5** with eq 1 gave $P_n = 4.3 \pm 0.5$, $T_1 = 520 \pm 50$ ns, and $k_1 = (2.5 \pm 0.4) \times 10^5$ s^{-1}. Thus, the phosphinoyl radicals **5** are produced in the W-band with a net polarization $P_n = 4.3 \pm 0.5$, which corresponds to an initial population difference P_nP_{eq}(W-band) $= 0.034 \pm 0.004$, and an initial W-band multiplet (E/A) CIDEP of $P_m = 4.3 \pm 0.7$, being also equivalent to 0.034 ± 0.005 in terms of the population difference.

Discussion

There are three main CIDEP mechanisms responsible for the production of the initial net and multiplet polarization in phosphinoyl radicals **2**, **4**, and **5** generated by photolysis of the investigated acylphosphine oxide photoinitiators: the triplet mechanism (TM) as well as ST_0 and ST_- radical pair mechanisms (ST_0 RPM and ST_- RPM) in the triplet (CO + PO) geminate radical pairs (Scheme 2). Therefore, the following relation is valid for the experimentally observed ratios, P_n/P_m (Table 1)

$$\frac{P_n}{P_m} = \frac{P(\mathrm{TM}) + P_n(\mathrm{ST}_0) - |P(\mathrm{ST\_})|}{P_m(\mathrm{ST}_0) + |P(\mathrm{ST\_})|} \qquad (2)$$

where P(TM) is the polarization arising from the TM, $P_n(ST_0)$ and $P_m(ST_0)$ are net and multiplet contributions from the ST_0 RPM, respectively, and $|P(ST_-)|$ is the absolute value of the polarization stemming from the ST_- RPM. Note that the ST_- RPM contributes equally to the net and multiplet polarization of phosphinoyl radicals, because the ST_- RPM results in emissive polarization of only the low-field EPR transition of phosphinoyl radicals (Results). To find out the TM polarization in absolute units, the values of all other contributions have to be obtained.

CIDEP Polarization Due to ST_0 RPM. In the W-band, only two CIDEP mechanisms are mainly responsible for formation of initial polarization of the phosphinoyl radicals, **2**, **4**, and **5**: TM and ST_0 RPM in triplet (CO + PO) geminate radical pairs (Scheme 2). The ST_- RPM contribution is insignificant and

can be neglected in the W-band (see below). The multiplet polarization is induced only by the ST_0 RPM. Therefore, in the W-band the absolute values of $P_m(ST_0)$ for the radicals **2**, **4**, and **5** are equal to the absolute values of the total multiplet polarization P_m. The absolute values of $P_m(ST_0)$ and $P_n(ST_0)$ contributions in all EPR bands can then be calculated by using their known dependences $f(Q)$ on the difference in Larmor frequencies Q. For the low- and high-field W-band EPR transitions of phosphinoyl radicals, the ST_0 RPM contributes in the following way

$$P_L^W(ST_0) = -f(Q_{LC}^W),\ P_H^W(ST_0) = f(Q_{CH}^W) \tag{3}$$

where Q_{LC}^W and Q_{CH}^W are the differences in Larmor frequencies between the W-band EPR transitions of the benzoyl radical (C) and the low (L)- and high (H)-field lines of the phosphinoyl radical, respectively. Taking half the sum and half the difference of the high- and low-field polarizations from eq 3, we can find the net and multiplet contributions of the ST_0 RPM in the W-band

$$P_n^W(ST_0) = \frac{f(Q_{CH}^W) - f(Q_{LC}^W)}{2} \tag{4}$$

$$P_m^W(ST_0) = \frac{f(Q_{CH}^W) + f(Q_{LC}^W)}{2} \tag{5}$$

If we write the function $f(Q)$ in its common form[8,9] $f(Q) = c\sqrt{Q}$ we get

$$P_n^W(ST_0) = \frac{c\Delta^W}{2} \quad P_m^W = \frac{c\sum^W}{2} \tag{6}$$

with $\Delta^W = \sqrt{Q_{CH}^W} - \sqrt{Q_{LC}^W}$ and $\Sigma^W = \sqrt{Q_{CH}^W} + \sqrt{Q_{LC}^W}$. From the W-band TREPR experiments, we know the absolute value of P_m^W (Results). Thus, the constant c is

$$c = \frac{2P_m^W}{\sum^W} \tag{7}$$

In a low viscosity solution, c is nearly independent of the microwave frequency.[8] Therefore, the absolute values of the net and multiplet ST_0 RPM contributions to the polarization in X-band (or S- or Q-band) can be easily obtained

$$P_n^X(ST_0) = \frac{c\Delta^X}{2} \quad \text{and} \quad P_m{}^X(ST_0) = \frac{c\sum^X}{2} \tag{8}$$

using the values of c from the W-band measurement (eq 7). The positions of the EPR resonances of the phosphinoyl radicals are[32]

$$B = \frac{A_0}{g\beta_e}\frac{1}{1-\alpha^2} \times \left(-M_I + \left\{M_I^2 + [1-\alpha^2]\left[\frac{1}{4\alpha^2} - \left(I + \frac{1}{2}\right)^2\right]\right\}^{1/2}\right) \tag{9}$$

with $\alpha = A_0/2h\nu_0$ in dependence on the EPR band frequency ν_0, A_0 the phosphorus hyperfine splitting in Hz, and $M_I = \pm 1/2$ the nuclear spin projection of the phosphorus for a given EPR transition. In this way, the values of Δ and Σ were obtained for all of the EPR bands, and the ST_0 RPM contributions in these bands were calculated and are collected in Table 2.

TABLE 2: Absolute Values of ST_0 RPM, ST_- RPM, and TM Contributions to the Initial Polarizations of Phosphinoyl Radicals, 2, 4, and 5 in Dependence on the EPR Frequency[a]

radical	contribution	S (2.8 GHz)	X (9.7 GHz)	Q (34.8 GHz)	W (95 GHz)
2	$P_n(ST_0)$	−4.3	−1.9	−3.0	−7.5
	$P_m(ST_0)$	44	43	43	43
	$\|P(ST\_)\|$	84 ± 31	22 ± 7	5.3 ± 1.6	1.7 ± 0.5
	P(TM)	220 ± 50	320 ± 50	130 ± 20	79 ± 12
4	$P_n(ST_0)$	−2.4	−1.3	−2.6	−7.2
	$P_m(ST_0)$	31	31	31	30
	$\|P(ST\_)\|$	61 ± 24	16 ± 5	3.9 ± 1.2	1.3 ± 0.3
	P(TM)	94 ± 25	90 ± 13	41 ± 6	29 ± 4
5	$P_n(ST_0)$	−2.5	−1.4	−3.0	−8.0
	$P_m(ST_0)$	35	34	34	34
	$\|P(ST\_)\|$	49 ± 18	13 ± 4	3.1 ± 0.9	1.0 ± 0.3
	P(TM)	210 ± 40	230 ± 40	63 ± 9	44 ± 6

[a] All values are multiplied by 10^3. The values given for $P_n(ST_0)$ and $P_m(ST_0)$ have an error of ±15%.

CIDEP Polarization Due to ST_- RPM. The ST_- RPM has been found previously to contribute to the X-band CIDEP spectra of dimethoxyphosphinoyl radicals ($A(P) \approx 70$ mT).[29] The generation of ST_- RPM CIDEP for phosphinoyl radicals, **2**, **4**, and **5**, with smaller hyperfine splitting ($A(P) \approx 25-40$ mT) was clearly seen in the S-band TREPR time profiles (Results). It contributes equally to both the initial net and multiplet polarization, since only $T_-(\alpha_N) \rightarrow S(\beta_N)$ transitions are induced by the isotropic hyperfine interaction in the region of the S and T_- terms crossing in the geminate RP of benzoyl and phosphinoyl radicals.[1]

To calculate the ST_- RPM contribution the analytical theory of Adrian[10,33] (and A. I. Shushin, spherical case, eq 28 in ref 34) has been used

$$|P(ST\_)| = \frac{\pi A^2 r_C}{4\omega_0 \lambda D} \tag{10}$$

where A is the hyperfine splitting, r_C the separation in the level crossing region, λ the range parameter in the exchange interaction (eq 12), $D = kT/6\pi\eta R$ the diffusion constant of an individual radical, and $\omega_0 = 2\pi\nu_0$. To calculate r_C as

$$r_C = d + \frac{1}{\lambda}\ln\left(\frac{2J_0}{\omega_0}\right) \tag{11}$$

the parameters J_0 and λ of the exchange interaction J

$$J = J_0 \exp(-\lambda(r - d)) \tag{12}$$

were taken as the average of the values reported for geminate RPs in the photolysis of **I** and other phosphine oxide compounds from $^{31}P-$CIDNP and SNP studies:[30,35] $J_0 = (3.0 \pm 1.4) \times 10^{10}$ rad/s, $1/\lambda = 0.06 \pm 0.02$ nm. The distance of closest approach d of geminate RPs in the photolysis of **I** was taken as 0.7 nm.[30,35] For the other compounds, d was taken as the sum of the radical radii calculated in spherical approximation:[36] $d(\mathbf{3} + \mathbf{4}) = 0.32 + 0.42 = 0.74$ nm, $d(\mathbf{1} + \mathbf{5}) = 0.33 + 0.39 = 0.72$ nm. The resulting absolute values of the ST_- RPM contributions, calculated with eq 10, are collected in Table 2. In the S-band, the estimated absolute values of the initial ST_- CIDEP are about two times larger than those of the ST_0 RPM contributions, whereas in the X-band they are two times lower and cannot always be clearly separated from the ST_0 RPM

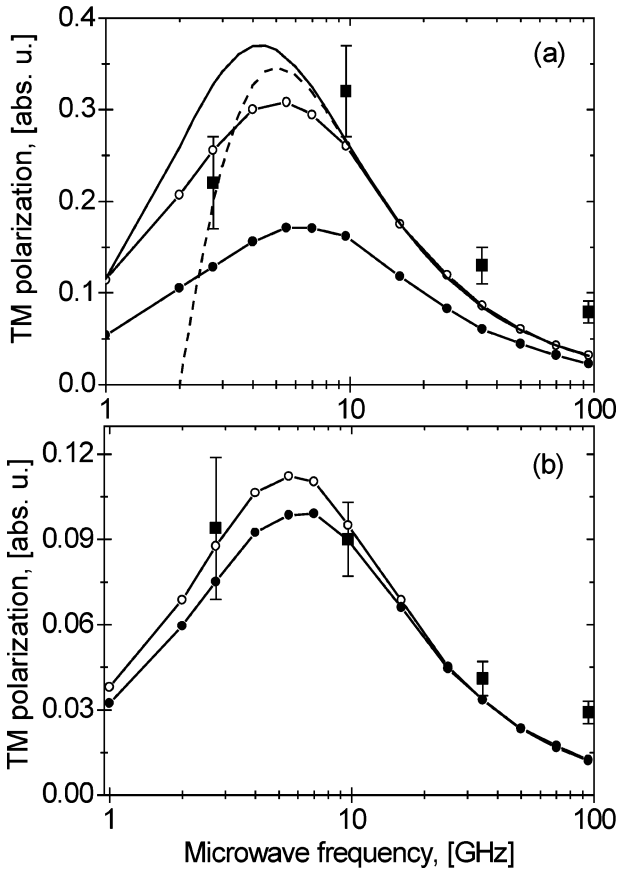

Figure 4. TM polarization of phosphinoyl radicals (■) (a) **2** and (b) **4** after photolysis of **I** and **II**, respectively, compared with the theoretical solutions: (●) numerical solution of the SLE (eq 13) using the triplet state parameters of (a) **I** and (b) **II** from Table 3; (○) fitted numerical solution of the SLE for (a) **I** ($\tau_c = 98$ ps and $w_z = 1$) and (b) **II** ($\tau_c = 86$ ps); (—) Atkins theory (eq 15) and (- - -) Pedersen−Freed analytical solution (see text) were calculated for **I** with the same parameters as were used for the fitted numerical solution (○).

CIDEP.[37] In the W-band, the ST$_-$ RPM contribution is several times smaller than the equilibrium polarization and can be neglected.

Despite the fact that Adrian's theory is a high field approximation, the conditions for its applicability were rather well satisfied for our systems, even in the S-band. The asymptotic parameter υ (eq 3 in ref 33) was equal or larger than 0.5 for all of the compounds. At $\upsilon \geq 0.5$, Adrian's analytical formula (eq 10) has been found to deviate less than 10% from the exact solution.[33] The applicability of the high field approximation at the S-band frequency has also been proven in a recent CIDEP study of the photolysis of **I** in low magnetic fields.[38]

CIDEP Polarization Due to TM. Because all CIDEP contributions due to the radical pair mechanism, $P_n(ST_0)$, $P_m(ST_0)$, and $P(ST_-)$, have been calculated in absolute units (Table 2), the values of the TM polarizations, P(TM), can be readily obtained in all EPR bands from the experimental P_n/P_m ratios (Table 1) and eq 2. The resulting absolute values of the TM polarizations for **2**, **4**, and **5** are collected in Table 2 and plotted as squares in Figures4 and 5 in dependence on the microwave frequency. The observed values of the TM polarization are extremely high. For example, the TM polarization of **2** exceeds the equilibrium polarization 410 times in the X-band (P_{eq}(X-band) $\approx 7.8 \times 10^{-4}$) and nearly 1000 times in the S-band (P_{eq}(S-band) $\approx 2.2 \times 10^{-4}$).

The magnetic field strength or microwave frequency υ_0 is an important parameter that determines the efficiency of spin

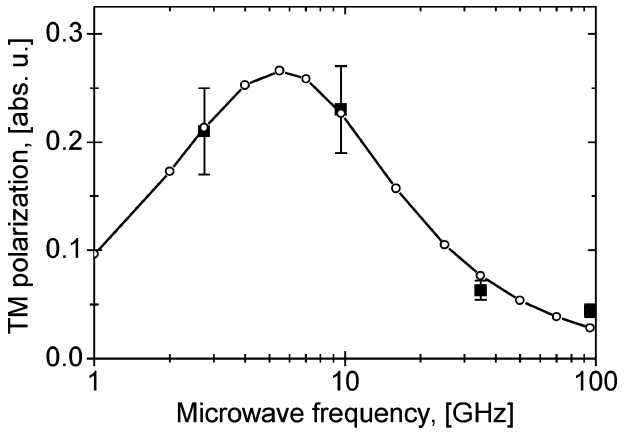

Figure 5. TM polarization of phosphinoyl radical **5** after photolysis of **III** (squares) compared with the numerical solution of the SLE (eq 13) (circles), calculated with the following set of parameters: $D_{ZFS} = 0.19$ cm^{-1}, $k_T = 9.6 \times 10^9$ s^{-1}, $w_z = 0.93$, and $\tau_c = 92$ ps.

polarization transfer from the molecular frame of the excited triplet molecule to the laboratory frame and then to the radicals. Qualitatively, the effect of microwave frequency on the size of the TM polarization is well understood[6,7] and has been nicely illustrated by a vector model.[39] For a maximum of TM polarization, the following conditions for $\omega_0 = 2\pi\upsilon_0$ have to be satisfied:[39] (i) $T_1^{-1} \leq k_T \leq \omega_0$, the electron spin precession frequency should be fast enough in comparison to the decay rate of the triplet molecule to radicals, k_T; (ii) $\omega_0 \approx D_{ZFS}$, ω_0 should be in the order of the zero-field splitting constant, D_{ZFS}; and (iii) $\tau_c^{-1} \leq \omega_0$, ω_0 should be faster than the reorientation diffusional motion of the triplet molecule. All of these three conditions, when satisfied, allow an effective transfer of initial molecular frame spin polarization of the triplet precursor to the radicals and, hence, lead to a maximum of TM polarization in the radicals. At very low microwave frequencies, $\omega_0 \leq \tau_c^{-1}$, k_T, and very high ones, $\omega_0 \gg D_{ZFS}$, the TM polarization vanishes. This behavior is qualitatively confirmed by our experiments with **I** and **III**. The experimental values of the TM CIDEP for these two compounds have a maximum at the X-band microwave frequency ($\upsilon_0 = 9.7$ GHz) (Table 2 and Figures 4 and 5).

To examine the TM polarization quantitatively, we used a similar approach to that proposed by Pedersen and Freed.[7] The spin evolution of the system is described by the stochastic Liouville equation (SLE) of the spin density matrix $\rho(t)$ of the excited triplet molecule. Assuming isotropic rotational diffusion the SLE for the TM reads

$$\frac{\partial\rho(t)}{\partial t} = D_R\nabla^2\rho(t) - i[\hat{H}, \rho(t)] - \frac{1}{2}\{k_T\hat{I}, \rho(t)\} \qquad (13)$$

with $D_R\nabla^2\rho(t)$ being the diffusion operator describing the action of the rotational diffusion on the evolution of the spin density matrix, D_R the rotational diffusion coefficient, $D_R = {}^1/_6\tau_c$, and τ_c the reorientational correlation time. $\hat{H}$ is the spin Hamiltonian of the triplet molecule comprising Zeeman and zero-field splitting interactions, and $k_T\hat{I}$ is the reaction operator accounting for the decomposition of the triplet molecule into radicals. The observable is the amount of triplet polarization transferred to the radicals

$$P_{TM} = \int_0^\infty k_T Tr(\hat{S}_Z^T\rho(t))\,dt \qquad (14)$$

The initial conditions for the SLE (eq 13) were chosen so that the triplet molecule at time $t = 0$ was polarized in the molecular

TABLE 3: Parameters of the Excited Triplet States of I and II from Refs 29 and 18

property	I	II
triplet lifetime		
$\tau_T = 1/k_T$ (ps)	~100	~300
zero-field splitting		
D_{ZFS} (cm^{-1})	0.1868 (7)	0.149 (1)
E_{ZFS} (cm^{-1})	0.00784 (6)	0.0140 (6)
initial population		
w_z	0.80 ± 0.25	0.66 ± 0.01
radii[a] (nm)	0.43	0.48
τ_c[a] (ps)	48	67

[a] Calculated values (see text).

frame having an initial density matrix $\rho(t = 0)$ diagonal in the zero-field state basis, T_x, T_y, T_z. Moreover, in the spherical approximation it is enough to solve eq 13 only for the case of an initial population of the T_z state equal to unity, $w_z = 1$ and $w_x = w_y = 0$. Then, to obtain the solution for an arbitrary initial population, this result has to be multiplied by a factor $r = w_z - (w_x + w_y)/2 = (3w_z - 1)/2$.[7] Thus, in our model, there are five parameters that determine the size of TM polarization: τ_c, υ_0, D_{ZFS}, k_T, and w_z. The SLE was integrated numerically using a Monte Carlo procedure, which is described in detail elsewhere.[40] For the numerical calculations, the parameters of the excited triplet states of **I** and **II** were taken from the literature.[29,18] They are collected in Table 3. The radii, R, of the triplet molecules were calculated in spherical approximation,[36] and their orientational correlation times were estimated with the Debye−Stokes formulas, $\tau_c = 4\pi\eta R^3/3kT$, where $\eta = 0.6$ cP is the viscosity of benzene at room temperature. These values are also collected in Table 3.

Figure 4a presents the experimental υ_0 dependence of the TM polarization of diphenylphosphinoyl radicals **2** (squares) and that calculated from the SLE (circles), using triplet state parameters of **I** from the literature (Table 3). The lower curve (filled circles) is calculated with an initial population of the T_z state equal to 0.8, $w_z = 0.8$. The upper curve (open circles) is the numerical solution fit to the experimental data. The variable parameters were the orientational correlation time τ_c and the initial population w_z, which was varied within the reported error limits, $w_z = 0.8 \pm 0.25$ (Table 3). In this case, the theory shows good agreement with the experimental data and explains well the dependence of the TM polarization on υ_0. The optimal values of the variable parameters resulting from least-squares fitting are $\tau_c = 98$ ps and $w_z = 1$. It is quite reasonable that the value obtained for the reorientational correlation time is not equal to the one estimated from the spherical approximation, $\tau_c = 48$ ps. Our assumption of isotropic rotational diffusion may be somewhat simplified. In reality, the rotational diffusion of the molecule will be very complex and an anisotropic process. Therefore, the rotational correlation time in our model should be considered as an effective parameter. It seems that the initial population of the T_z state is close to unity, $w_z \approx 1$. This is necessary to explain the large TM polarization observed experimentally in the X-band. In Figure 4a, the fitted numerical solution is compared with two analytical theories given by Atkins and Evans[6] (solid line) and by Pedersen and Freed[7] (dashed line). In the case of isotropic rotational diffusion (spherically symmetric triplet molecule, $E_{ZFS} = 0$), the Atkins formula reads

$$P_{TM}^{A} = \frac{4}{3} P_{eq} + \left(S_Z^* - \frac{4}{3} P_{eq}\right) \frac{k_T T_1}{1 + k_T T_1} \qquad (15)$$

where

$$S_Z^* = \frac{4}{15} \omega_0 r D_{ZFS} \left(\frac{1}{\omega_0^2 + (k_T + \tau_c^{-1})^2} + \frac{4}{4\omega_0^2 + (k_T + \tau_c^{-1})^2} \right)$$

$$\frac{1}{T_1} = \frac{2}{15} D_{ZFS}^2 \frac{1}{\tau_c} \left(\frac{1}{\tau_c^{-2} + \omega_0^2} + \frac{4}{\tau_c^{-2} + 4\omega_0^2} \right)$$

and factor $r = w_z - (w_x + w_y)/2 = (3w_z - 1)/2$. In Figure 4a, the plotted Atkins solution (eq 15) was calculated using the same parameters as the fitted numerical one. In the X-band and higher frequencies, Atkins theory shows a very good agreement with the numerical solution, but in the region of microwave frequencies between the S- and X-bands, it deviates from the exact solution by about 25%. This is because the applicability regime of the Atkins solution partially breaks. Equation 15 has been obtained for fast diffusional motion, when the reorientational correlation time is much shorter than the reciprocal zero-field splitting constant, the triplet state lifetime, and the Larmor period,[3] $\tau_c \ll 1/D_{ZFS}$, $1/k_T$, $1/\omega_0$. In the case of compound **I**, these conditions are not satisfied because $\tau_c \approx 1/k_T$ and $\tau_c < 1/D_{ZFS}$. The analytical formula of Pedersen and Freed (eq 34 in ref 7) is in good agreement with the numerical solution only in X- and higher bands. It is applicable under the conditions (eq 38 in ref 7): $D_{ZFS}^2 \le [\omega_0^2 + \tau_c^{-2}]/2$.

The triplet state parameters of compound **II** are also known (Table 3). Figure 4b presents the experimental υ_0 dependence of the TM polarization of phosphinoyl radical **4** produced in the photolysis of **II** (squares) and the numerically calculated solutions of the SLE (eq 13) (circles). The solid circles are numerical solutions using triplet parameters of **II** from the literature and a reorientational correlation time calculated in spherical approximation (Table 3). Even without fitting, the numerical solution is in very good agreement with the experiment. The open circles characterize the fitted numerical solution with only one free variable. The value of the reorientational correlation time τ_c was varied, and the optimal value of it was found equal to 86 ps. The deviations by a factor of 2 between the theoretical and the experimental W-band data for **I** and **II** (Figure 4) possibly arise from the anisotropy of the rotational diffusion of the triplet molecule, which is not captured by our model.

For the last compound, **III**, the triplet parameters are not known. We used our experimental data of the TM polarization in phosphinoyl radical **5** and the numerical solution of the SLE to obtain these unknown triplet parameters. A reorientational correlation time of 92 ps was estimated from the optimal values obtained for the two previous compounds and was kept fixed. Free parameters were fitted for the zero-field splitting D_{ZFS}, the first-order decomposition rate constant of the triplet state k_T, and the initial population w_z. The following estimations for the unknown parameters were obtained: $0.169\ cm^{-1} \le D_{ZFS} \le 0.195\ cm^{-1}$, $5 \times 10^9\ s^{-1} \le k_T \le 2.5 \times 10^{10}\ s^{-1}$ (excited triplet state lifetime, 40 ps $\le \tau_T = 1/k_T \le$ 200 ps), and $0.92 \le w_z \le 1$. Variations in the reorientational correlation time τ_c within 15% did not change the presented estimations of the triplet state parameters of **III**. The obtained parameters are reasonable and close to the values for the first two compounds. In Figure 5, the experimental data for **5** (squares) and the numerical solution (circles) of the SLE (eq 13) are presented with the parameter set: $D_{ZFS} = 0.19\ cm^{-1}$, $k_T = 9.6 \times 10^9\ s^{-1}$, $w_z = 0.93$, and $\tau_c = 92$ ps. This example demonstrates, first, the consistency of our experimental results and theory and, second, how the

observation of CIDEP in radicals can give access to parameters of their excited triplet precursor.

Conclusion

The CIDEP pattern was studied in phosphinoyl radicals produced by photolysis of three acylphosphine oxide photoinitiators, diphenyl-2,4,6-trimethylbenzoyl phosphine oxide, bis-(2,6-dimethoxybenzoyl)-(2,4,4-trimethylpentyl) phosphine oxide, and bis(2,4,6-trimethylbenzoyl) phenylphospine oxide. Strong spin polarizations of the radicals are found to be generated by the triplet mechanism as well as by ST_0 and ST_- radical pair mechanisms. They change in dependence on the microwave frequency and were analyzed in a multifrequency time-resolved EPR investigation at both high and low microwave frequencies, covering S- (2.8 GHz, 0.1 T), X- (9.7 GHz, 0.34 T), Q- (34.8 GHz, 1.2 T), and W- (95 GHz, 3.4 T) bands. The TM polarization dependence on microwave frequency was obtained in absolute units and explained quantitatively by a numerical solution of the stochastic Liouville equation (SLE) following the Pedersen and Freed approach.[7] The good agreement between the experimental results and the SLE solution gives quantitative proof for the correctness of the theoretical model for the TM. The approximate analytical formulas for the TM polarization given by Atkins and Evans[6] and Pedersen and Freed[7] are valid only at high microwave frequencies/magnetic fields, though the Atkins approximation remains qualitatively correct for the investigated systems also at low microwave frequencies.

Parameters of the excited triplet state of bis(2,4,6-trimethylbenzoyl) phenylphospine oxide were estimated from the dependence of its TM polarization on microwave frequency.

Acknowledgment. Helpful discussions with A. I. Shushin and financial support by the Swiss National Foundation for Scientific Research are gratefully acknowledged.

Supporting Information Available: EPR spectra and time profiles of phosphinoyl radicals **4** and **5** recorded after photolysis of **II** and **III**, respectively, in benzene at room temperature. This material is available free of charge via the Internet at http://pubs.acs.org.

References and Notes

(1) Salikhov, K. M.; Molin, Y. N.; Sagdeev, R. Z.; Buchachenko, A. L. *Spin Polarization and Magnetic Effects in Radical Reactions*; Molin, Y. N., Ed.; Elsevier: Amsterdam, 1984.

(2) McLauchlan, K. A. In *Modern Pulsed and Continuous-Wave Electron Spin Resonance*; Kevan, L., Bowman, M. K., Eds.; Wiley: New York, 1990; pp 285−363.

(3) Steiner, U. E.; Ulrich, T. *Chem. Rev.* **1989**, *89*, 51.

(4) Nagakura, S.; Hayashi, H.; Azumi, T. *Dynamic Spin Chemistry: Magnetic Controls and Spin Dynamics of Chemical Reactions*; Kodansha Ltd.: Tokyo, 1998.

(5) van Willigen, H. In *Molecular and Supramolecular Photochemistry*; Ramamurthy, V., Schanze, K. S., Eds.; Dekker: New York, 2001; Vol. 6, pp 197−247.

(6) Atkins, P. W.; Evans, G. T. *Mol. Phys.* **1974**, *27*, 1633.

(7) Pedersen, J. B.; Freed, J. H. *J. Chem. Phys.* **1975**, *62*, 1706.

(8) Freed, J. H.; Pedersen, J. B. *Adv. Magn. Reson.* **1976**, *8*, 1.

(9) Adrian, F. J. *Chem. Phys. Lett.* **1981**, *80*, 106.

(10) Adrian, F. J.; Monchick, L. *J. Chem. Phys.* **1979**, *71*, 2600.

(11) Blätter, C.; Jent, F.; Paul, H. *Chem. Phys. Lett.* **1990**, *166*, 375.

(12) Shushin, A. I. *J. Chem. Phys.* **1993**, *99*, 8723.

(13) Closs, G. L.; Forbes, M. D. E.; Norris, J. R. *J. Phys. Chem.* **1987**, *91*, 3592.

(14) van der Waals, J. H.; de Groot, M. S. In *The Triplet State*; Zahan, A., Ed.; Cambridge University Press: Cambridge, 1967.

(15) Ohara, K.; Terazima, M.; Hirota, N. *J. Phys. Chem.* **1995**, *99*, 17814.

(16) Rutsch, W.; Dietliker, K.; Leppard, D.; Koehler, M.; Misev, L.; Kolczak, U.; Rist, G. *Prog. Org. Coat.* **1996**, *27*, 227 and references therein.

(17) Kolczak, U.; Rist, G.; Dietliker, K.; Wirz, J. *J. Am. Chem. Soc.* **1996**, *118*, 6477 and references therein.

(18) Jockusch, S.; Koptyug, I. V.; McGarry, P. F.; Sluggett, G. W.; Turro, N. J.; Watkins, D. W. *J. Am. Chem. Soc.* **1997**, *119*, 11495.

(19) Sluggett, G. W.; Turro, C.; George, M. G.; Koptyug, I. V.; Turro, N. J. *J. Am. Chem. Soc.* **1995**, *117*, 5148 and references therein.

(20) Kamachi, M.; Kuwata, K.; Sumiyoshi, T.; Schnabel, W. *J. Chem. Soc., Perkin Trans. 2* **1988**, 961.

(21) Jockusch, S.; Turro, N. J. *J. Am. Chem. Soc.* **1998**, *120*, 11773.

(22) Gatlik, I.; Rzadek, P.; Gescheidt, G.; Rist, G.; Hellrung, B.; Wirz, J.; Dietliker, K.; Hug, G.; Kunz, M.; Wolf, J.-P. *J. Am. Chem. Soc.* **1999**, *121*, 8332.

(23) Baxter, J. E.; Davidson, R. S.; Hageman, H. J.; McLauchlan, K.; Stevens, D. G. *J. Chem. Soc., Chem. Commun.* **1987**, 74.

(24) Savitsky, A. N.; Galander, M.; Möbius, K. *Chem. Phys. Lett.* **2001**, *340*, 458.

(25) Kausche, T.; Säuberlich, J.; Trobitzsch, E.; Beckert, D.; Dinse, K.-P. *Chem. Phys.* **1996**, *208*, 375.

(26) Stephenson, D. S. *Nucl. Magn. Reson. Spectrosc.* **1988**, *20*, 515.

(27) Jent, F.; Paul, H. *Chem. Phys. Lett.* **1987**, *160*, 632.

(28) Shushin, A. I. *Chem. Phys.* **1990**, *144*, 201 and 223 and references therein.

(29) Koptyug, I. V.; Ghatlia, N. D.; Sluggett, G. W.; Turro, N. J.; Ganapathy, S.; Bentrude, W. G. *J. Am. Chem. Soc.* **1995**, *117*, 9486.

(30) Ananchenko, G. S.; Purtov, P. A.; Bagryanskaya, E. G.; Sagdeev, R. Z. *J. Phys. Chem. A* **1997**, *101*, 3848.

(31) Fedin, M. V.; Purtov, P. A.; Bagryanskaya, E. G. *J. Chem. Phys.* **2003**, *118*, 192.

(32) Weil, J. A.; Bolton, J. R.; Wertz, J. E. *Electron Paramagnetic Resonance: Elementary Theory and Practical Applications*; Wiley: New York, 1994; p 460.

(33) Adrian, F. J.; Monchick, L. *J. Chem. Phys.* **1980**, *72*, 5786.

(34) Shushin, A. I. *Chem. Phys. Lett.* **1995**, *237*, 177.

(35) Ananchenko, G. S.; Bagryanskaya, E. G.; Tarasov, V. F.; Sagdeev, R. Z.; Paul, H. *Chem. Phys. Lett.* **1996**, *255*, 267.

(36) Edward, J. T. *J. Chem. Educ.* **1970**, *47*, 261.

(37) Slugget, G. W.; McGarry, P. F.; Koptyug, I. V.; Turro, N. J. *J. Am. Chem. Soc.* **1996**, *118*, 7367.

(38) Fedin, M. V.; Yashiro, H.; Purtov, P. A.; Bagryanskaya, E. G.; Forbes, M. D. E. *Mol. Phys.* **2002**, *100*, 1171.

(39) Hore, P. J. *Chem. Phys. Lett.* **1980**, *69*, 563.

(40) Makarov, T. N. Ph.D. Thesis; Zurich, 2004.